Colloid Polym Sci (2005) 284: 309–316
DOI 10.1007/s00396-005-1380-8

ORIGINAL CONTRIBUTION

Saziye Uğur
Önder Pekcan

Time evolution of film formation from polystyrene particles: a percolation approach

Received: 5 September 2004
Accepted: 20 May 2005
Published online: 15 September 2005

Önder Pekcan (✉)
Department of Physics, Isık University,
34398 Maslak, Istanbul, Turkey
E-mail: pekcan@isikun.edu.tr
Tel.: +90-216-5287180
Fax: +90-216-7121474

Saziye Uğur
Department of Physics,
Istanbul Technical University,
34469 Maslak, Istanbul, Turkey
Tel.: +90-212-2853213
Fax: +90-212-2856386

Abstract This work reports the film formation process from surfactant-free polystyrene (PS) latex particles. Steady state fluorescence and photon transmission techniques were used to study the evolution of film formation. The films were prepared from fluorescein (*F*)-labeled PS latex particles at room temperature and annealed in 2.5-min-time intervals above the glass transition temperature (T_g) of PS. Fluorescence intensity (I_F) from *F* was measured after each annealing step to monitor the stages of film formation. Evolution of transparency of latex films was monitored by using the photon transmission intensity, I_{tr}. Drastic increase in I_{tr} and I_F above the critical annealing times, t_r and t_c, respectively, were attributed to the percolation behavior of the PS material. Critical exponents, β, of percolation clusters were measured and found to be around 0.31 and 0.37 for I_{tr} and I_F measurement, respectively, which were attributed to the site percolation model.

Keywords Latex film · Percolation · Transmitted light · Fluorescence · Polystyrene particles

Introduction

The interest in polymer latex film formation has grown enormously in recent years due to the need to find alternatives for solvent-based systems with their adverse environmental impact. This is manifest in paint industry where traditional solvent-based paints are seen as environmentally unfriendly while increasingly good quality of waterborne coatings allow solvent-based coatings to be substituted. In the past few years water-based polymer latexes have gained more attention beyond their current uses in paints, adhesives, coating, pharmaceuticals, printing inks, etc., than conventional solvent-based systems mainly because of environmental restraints. Several factors are experimentally known to influence latex film formation: the molecular weight and its distribution [1, 2], stabilizers [3] and surfactants [4]. In addition, the quality of these films, for a given molecular weight, depends on the annealing time and annealing temperature [5–8].

The latex film forms due to the ''coalescence'' (i.e. compaction, deformation, cohesion and polymer chain interdiffusion) of individual latex particles. The term ''latex film'' normally refers to a film formed from soft latex particles (T_g below room temperature) where the forces accompanying the evaporation of the solvent are sufficient to compress and deform the particles into transparent, void-free film. However, latex films can also be obtained by compression molding of a film of dried latex powder composed of relatively hard polymers, such as polystyrene (PS) or poly(methyl methacrylate) (PMMA) that has T_g above room temperature. Aqueous dispersion of soft latex particles is called low-it T_g, while nonaqueous dispersion of hard polymer particles is generally referred to as high-it T_g. High-it T_g latex particles remain essentially discrete and undeformed

during drying. The mechanical properties of such films can be evolved after all the solvent has evaporated by an annealing process, which first leads to void closure and then to inter-diffusion of chains across particle–particle boundaries.

Three steps can be distinguished during the film formation process from low-it T_g particles that have been observed experimentally [9]: in the first step, colloid concentration increases as water evaporates and a uniform shrinkage of the interparticle distance occurs and the voids are gradually filled by particle sliding, until a dense packing of spheres is obtained. In the second step, particle deformation due to the evaporation of the bounded water occurs. Finally, in the third step, due to interdiffusion of macromolecules, the mechanical strength increases and the water permeability of the film decreases. Under certain conditions the polymer chains can diffuse through the particle boundaries and a homogeneous, continuous film is formed. However, high-it T_g particles follow a different line of film formation processes. Particles form a powder after evaporation of water. Annealing of this powder at first causes void closure, then further annealing promotes the healing and interdiffusion processes, respectively.

Various experimental techniques have been used to study latex film formation stages and mechanisms, which are given below. Small-angle neutron scattering (SANS) has been used to study latex film formation at molecular level. Extensive studies using SANS have been done by Sperling and co-workers [10] on compression-molded PS film. Direct non radiant energy transfer (DET) method has been employed to investigate the film formation process from dye-labeled polymeric particles [11–13]. Steady state fluorescence (SSF) technique combined with DET has been used to examine healing and interdiffusion processes in the dye labeled PMMA latex systems [14, 15]. Photon transmission method has been used to study latex film formation from PMMA and PS particles, using the UV-visible (UVV) technique as a function of temperature and time [16–18].

This study introduces a new approach to film formation from latex particles. This new concept is based on the percolation model associated with a paper by Broadbent and Hammersly [19] where the general situation is a fluid spreading randomly through a medium. The spreading of blight from tree to tree in an orchard was also discussed by the same authors when the trees are planted at square lattice intersections. The percolation threshold, p_c, for this problem is around 0.6 for the so called "site percolation" on a square lattice. In another example, water seeps into the cracks and fractures of a rock formation [20]. Percolation also offers a simple and yet detailed picture from which one may seek to understand gelation, imagining monomers as occupying the vertices of a periodic lattice [21, 22]. The gel point can then be identified with the percolation threshold p_c, where the incipient infinite cluster starts to form.

In this work, we studied film formation from surfactant-free PS latex particles as a function of time by monitoring the fluorescence emission intensity (I_F) from a dye using SSF technique. Latex films were prepared by annealing latexes above the glass transition temperature

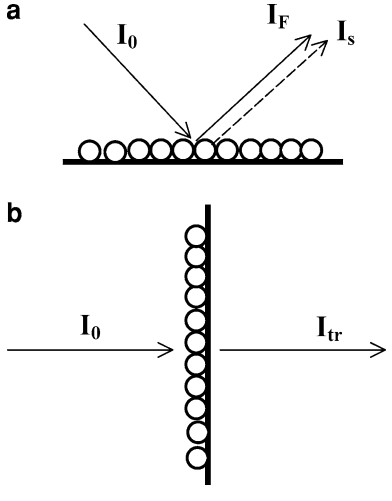

Fig. 1 Schematic illustration of sample position and incident light (I_0), **a** Emission (I_F) and scattering (I_s) intensities, **b**transmitted light intensity (I_{tr})

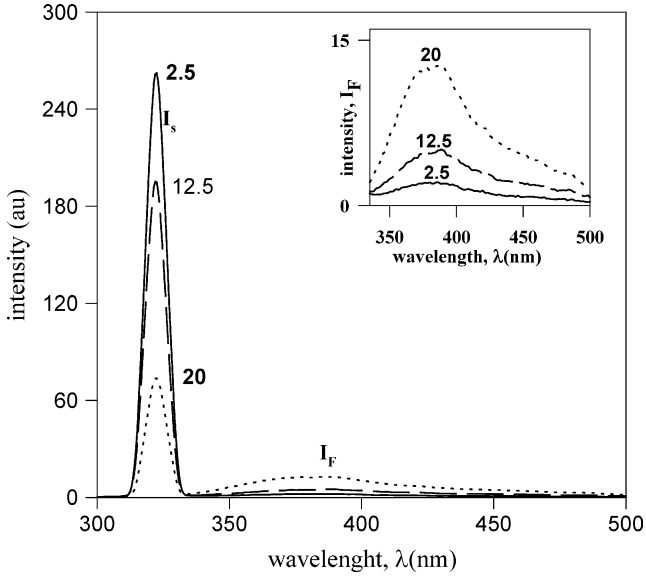

Fig. 2 Emission spectra of PS latex film after annealing at 130°C in various annealing time intervals. Numbers on each curve present the time intervals in minute. The sample is excited at 323 nm

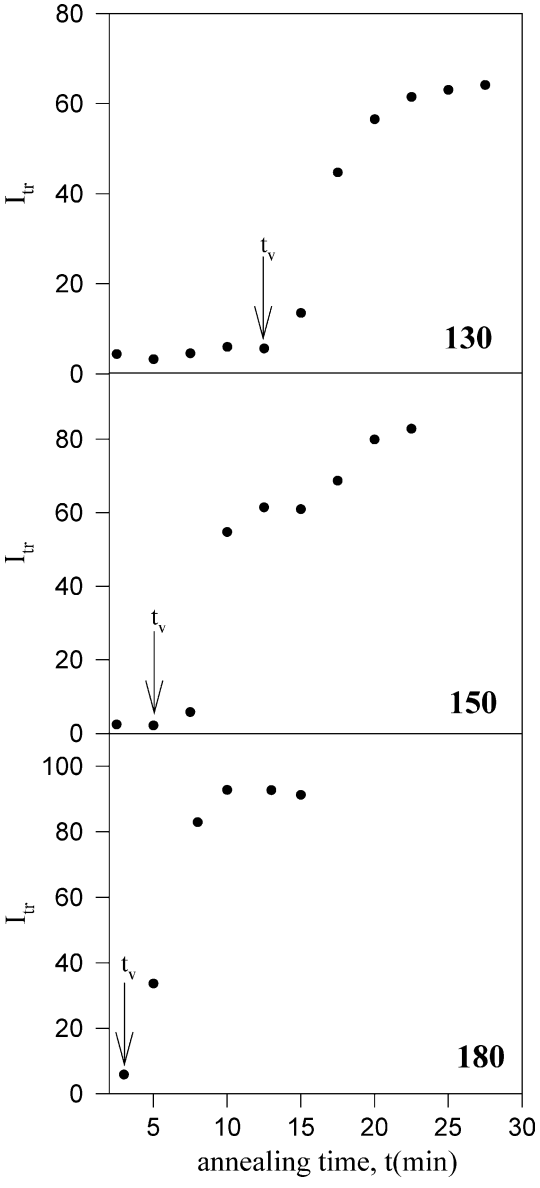

Fig. 3 Plot of I_{tr} versus annealing time for the films annealed at **a** 130°C, **b**150°C and **c** 180°C

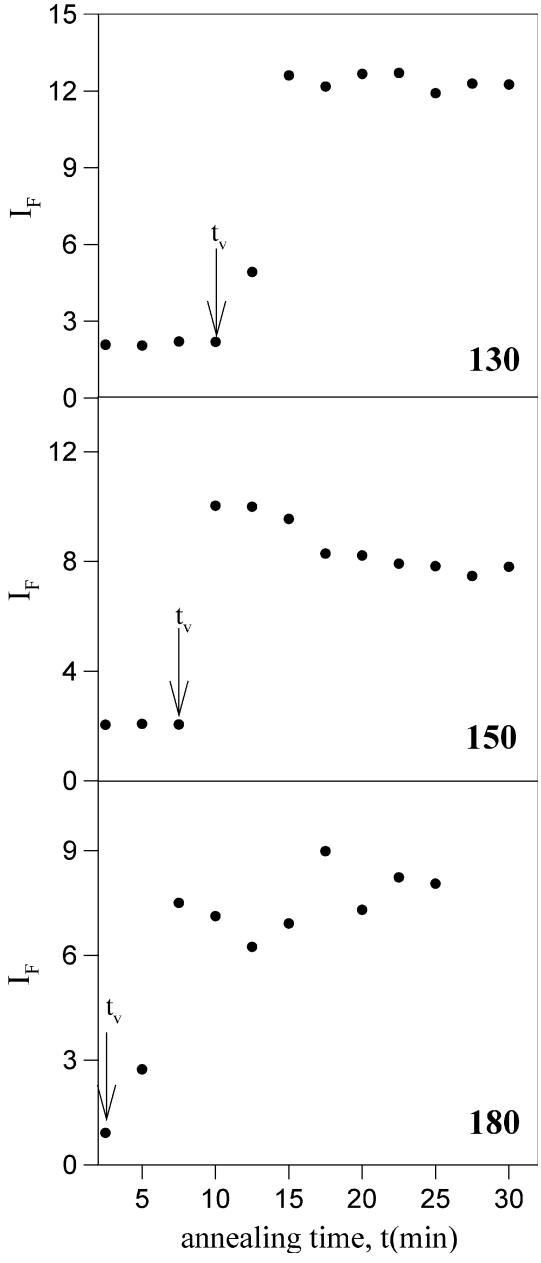

Fig. 4 Plot of I_F versus annealing time for the films annealed at **a** 130°C, **b**150°C and **c** 180°C

of PS ranging from 130 to 180°C for 2.5-min-time intervals. Transmitted photon intensity, I_{tr} was also monitored to study the evolution of transparency. Isothermal experiments were performed by annealing latex films in equal time intervals, then the direct fluorescence emission was monitored. Increase in I_F and I_{tr} intensities by increasing the number of annealing time intervals was attributed to percolation of PS material during the film formation process. It is observed that all $I_F$and I_{tr} intensities increased dramatically above specific annealing times called critical times, t_c and t_r, respectively at all temperatures.

Theoretical considerations

The most interesting feature of the percolation phenomenon is the existence of a percolation threshold, p_c below which the spreading process is confined to a finite region [19]. A typical problem of practical interest is the spread of water displacing oil in porous rocks where neighboring pores are connected by small capillary channels [23]. If there is no oil in the system, water in-

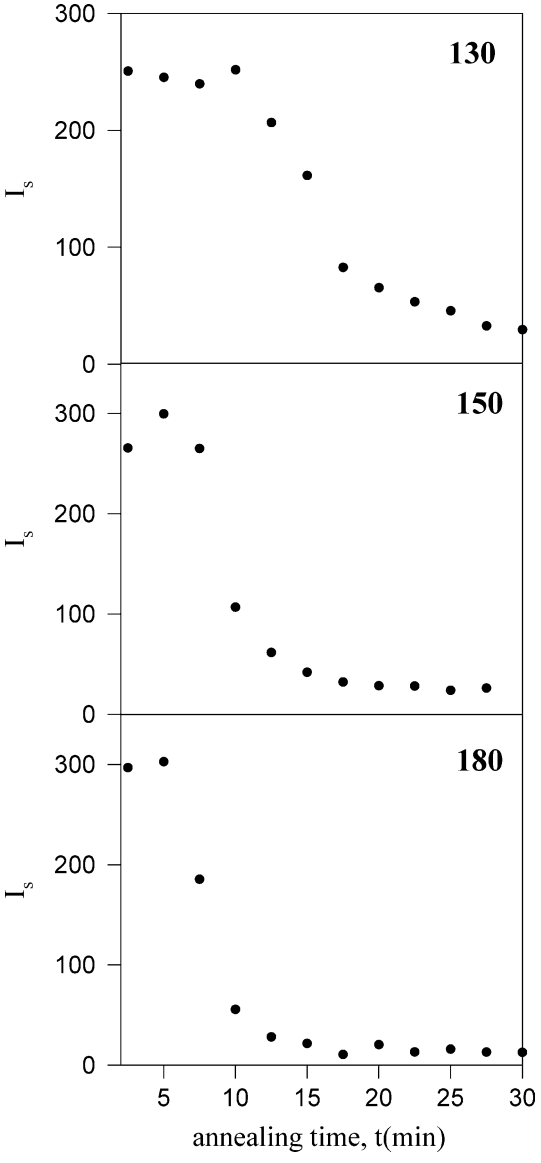

Fig. 5 Plot of I_s versus annealing time for the films annealed at **a** 130°C, **b**150°C and **c**180°C

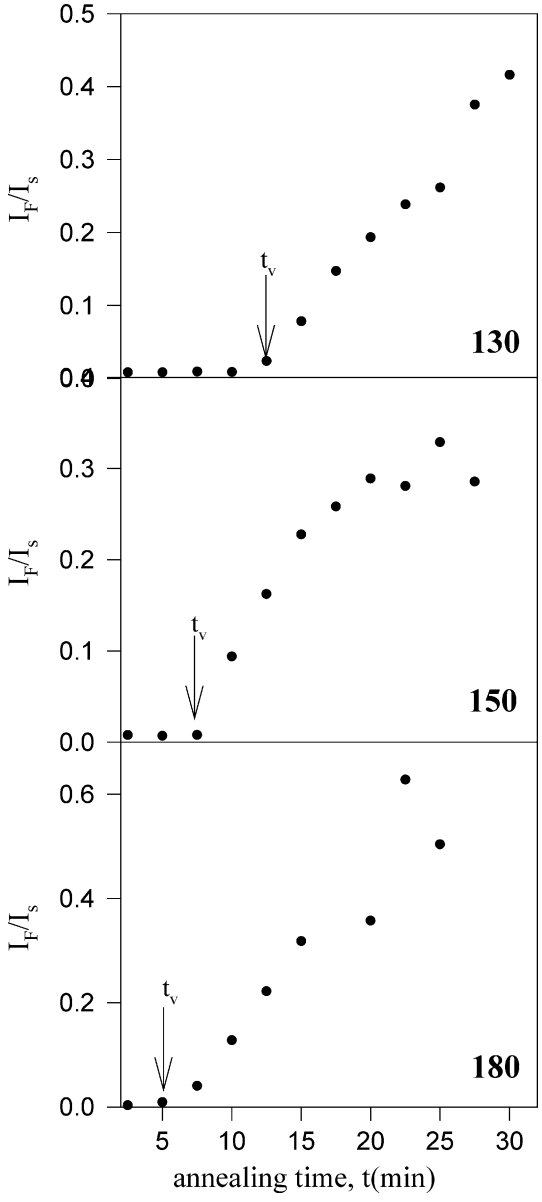

Fig. 6 Plot of I_F/I_s versus annealing time for the films annealed at **a** 130°C, **b**150°C and **c** 180°C

jected into any given pore can only invade another pore through capillary channels or "bonds". The pores are "sites" connected to the chosen center of injection called a "cluster". When the occupation probability, p, reaches 0.6, the largest cluster spans the lattice connecting the left and right edges to the bottom edge, which is called "percolation cluster". The percolation probability, $P_\infty(p)$, is defined as the probability that water injection at a site, chosen at random, will wet infinitely many pores. Here it should be noted that the probability of having a pore at all the site where water injection is attempted is p.

Extensive simulations and theoretical work have shown that the percolation probability vanishes as a power-law near p_c:

$$p_\infty(p) \approx (p - p_c)^\beta \tag{1}$$

for $p > p_c$, and $p \rightarrow p_c$. The exponents β and p_c in a simple cubic lattice are 0.4 and 0.31, respectively.

The probability, $P_N(p)$, of a site belonging to the largest cluster in $L \times L$ lattice with N pores is given by

$$P_N(p) = \frac{M(L)}{L^2} \tag{2}$$

where $M(L)$ is the number of sites in the largest cluster. For $p > p_c$ and $L \rightarrow \infty$ Eq. 2 produces $P_\infty(p)$, which is

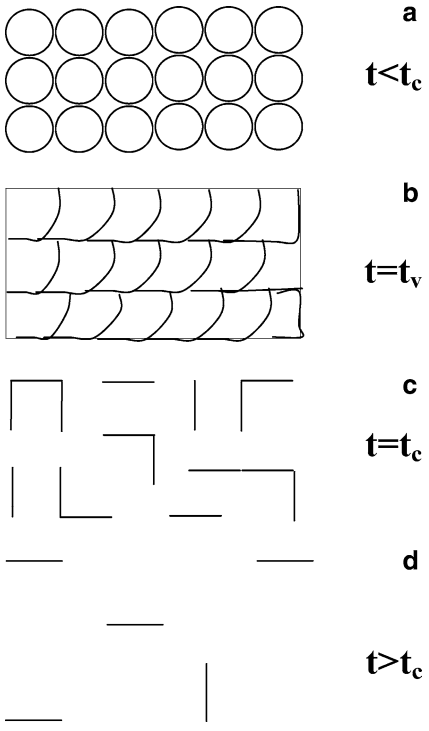

Fig. 7 Schematic illustration of the film formation from latex particles; **(a)**, **(b)**, **(c)**and **(d)** correspond to the film formation stages such as **a** film in powder form, **b** film after void closure process is ended, **c** percolation cluster is formed and **d**transparent film

simply the density of the sites that belong to the percolating cluster.

Experimental

Slightly cross-linked PS latex was produced via the surfactant free emulsion polymerization process. The polymerization was performed batch-wise using a thermostated reactor equipped with a condenser, thermocouple, mechanical stirring paddle and nitrogen inlet. The agitation rate was 300 rpm and the polymerization temperature was controlled at 70°C. Water (50 ml), styrene (5 g) and the crosslinker (0.006 g of fluorescent Fluorescein dimethacrylate, PolyFluor 511) were first mixed in the polymerization reactor and when the temperature was constant (at 70°C), KPS initiator (0.06 g), dissolved in small amount of water (3 ml), was introduced in order to induce styrene polymerization. The polymerization was conduced for 17 h. Molecular weight (M_w) of PS was obtained from GPC and measured as 4.55×10^4 g/mol. The poly-dispersion of the corresponding PS was 3.63. The particle size was measured from SEM pictures and found to be around 900 nm. SEM micrographs were taken at 10—15 kV in a JEOL JSM microscope. A Hummer VII sputtering system was used for gold coating of latex films.

Films were prepared from the dispersion of particles by placing different number of drops on a glass plate of

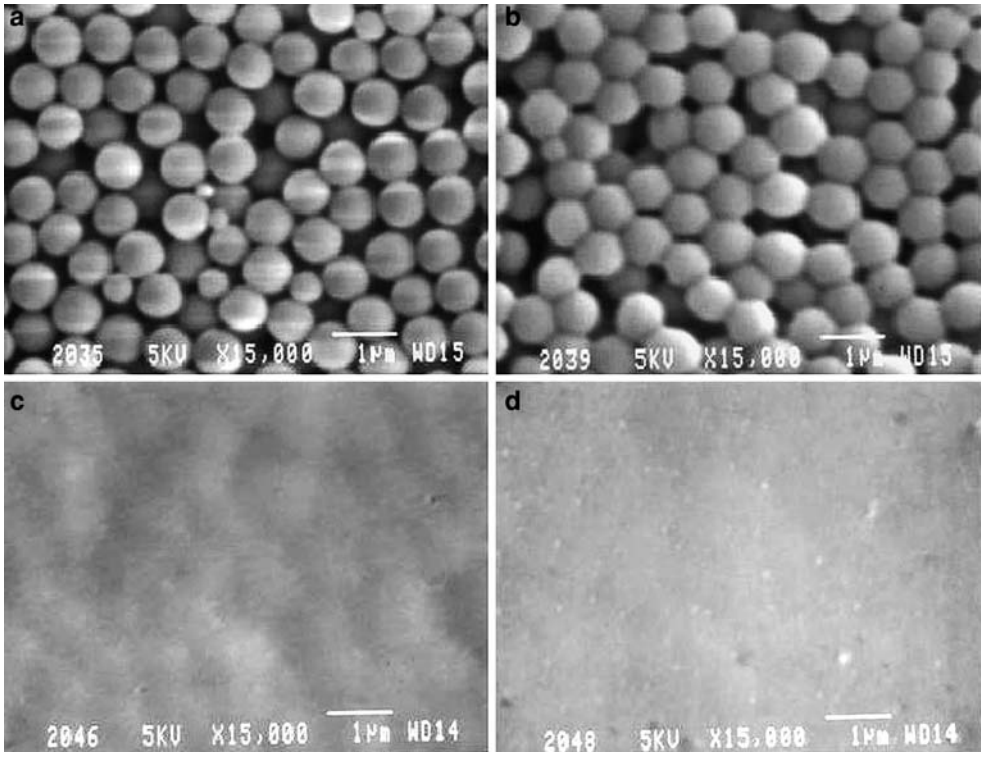

Fig. 8 SEM micrographs of PS latex film annealed at **a** 130°C, **b** 140°C, **c**150°C and **d**170°C temperatures for 2.5-min-time interval

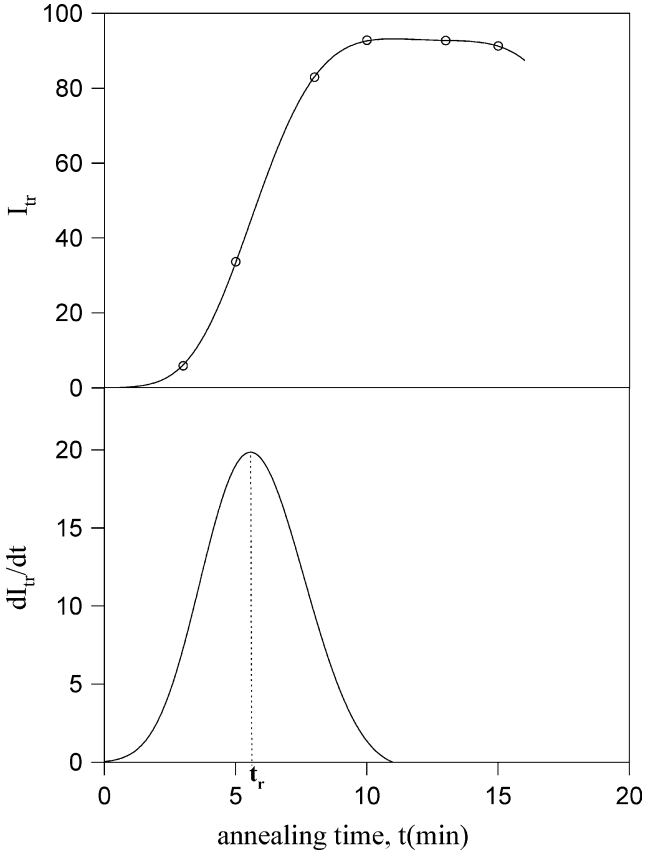

Fig. 9 Plot of time derivative of I_{tr} and its position at the time axis, $t_r$for the sample annealed at 180°C

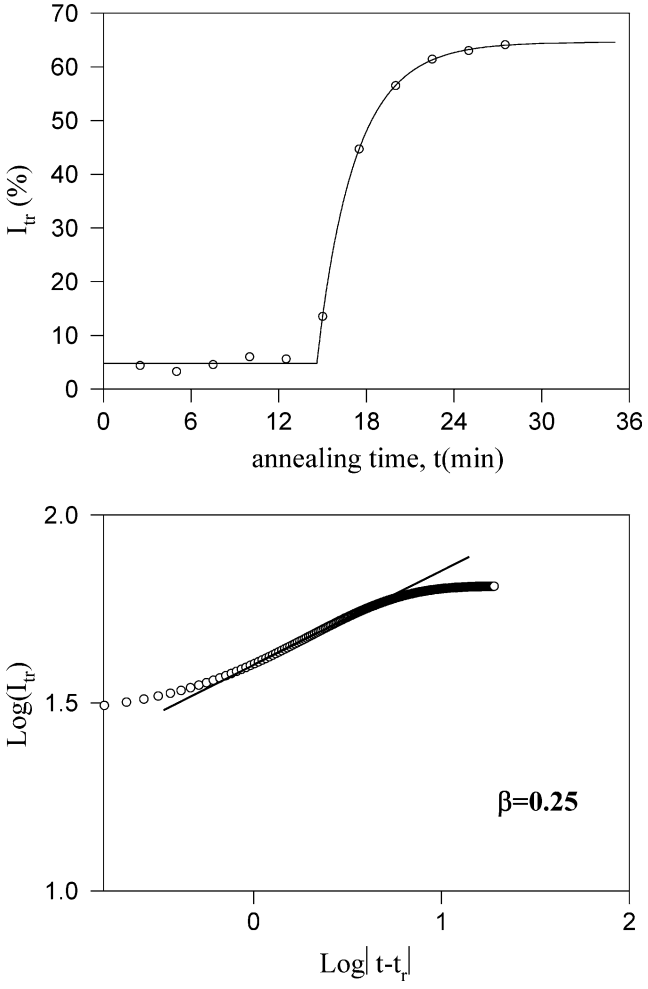

Fig. 10 Log–Log plot of I_{tr} versus $|t - t_r|$ for sample annealed at 130°C for 2.5-min time interval

0.8×2.5 cm and allowing the water to evaporate. Thickness of the films was measured by weighting them before and after dissolution, and estimated at around 20 μm. Then the samples were separately annealed in an oven above $T_g$of PS for 2.5 min time intervals at 130, 140, 150, 160, 170 and 180°C. For example, a given sample was annealed for 2.5-min intervals up to total 30 min, at 130°C. Similar procedure was repeated for the other sample at a given temperature. The temperatures was maintained within ±2°C during annealing.

After annealing, each sample was placed in the solid surface accessory of a Perkin-Elmer Model LS-50 fluorescence spectrometer. Fluorescein was excited at 323 nm and scattered light and fluorescence emission were detected at 300 and 500 nm. All measurements were carried out in the front-face position at room temperature. Slit widths were kept at 8 nm during all SSF measurements. The sample position, incident I_0 and scattered light, and I_s intensities are shown in Fig. 1a, where I_F is the emission of fluorescein intensity from fluorescein.

Photon transmission experiments were carried out using model DU 530 Life Science UVV spectrometer from Beckman. The transmittances of the films were detected between 300 and 400 nm. A glass plate was used as a standard for all UVV experiments and measurements were carried out at room temperature after each annealing processes. The sample position and the transmitted light intensity, I_{tr} are presented in Fig. 1b.

Table 1 Experimentally measured critical exponents, β for the films annealed at various temperatures at 2.5 min-time intervals

Temp(°C)	130	140	150	160	170	180	Avarage
I_{tr}	0.25	0.29	0.30	0.40	0.28	0.31	0.31 ± 0.05
I_c	0.48	0.31	0.44	0.25	0.39	0.34	0.37 ± 0.08

Results and discussion

The fluorescence emission spectra of latex film annealed at 130°C in different total annealing times and excited at

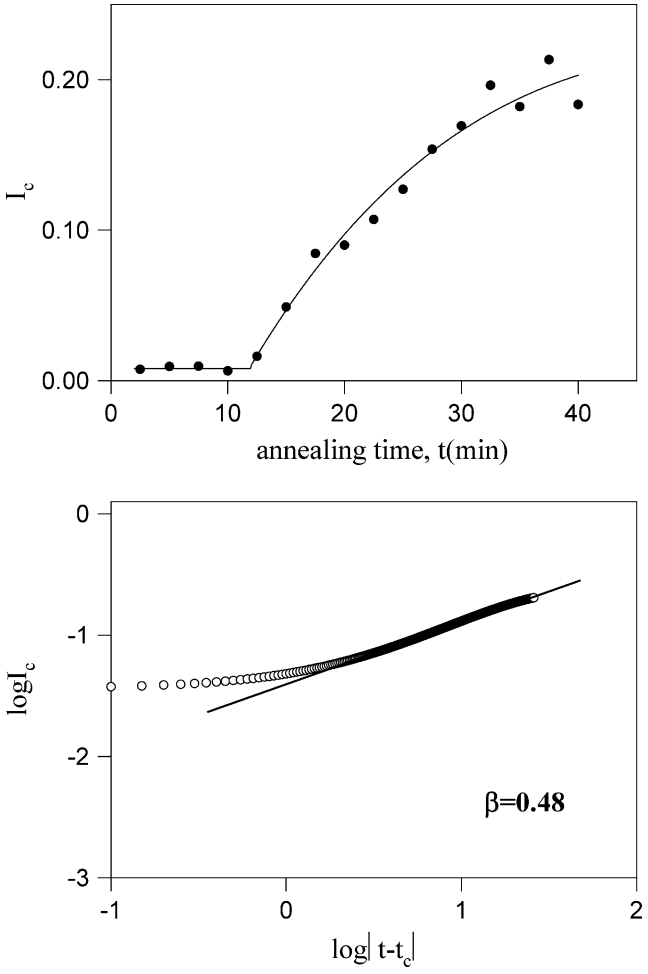

Fig. 11 Log–Log plot of I_c versus $|t - t_c|$ for sample annealed at 130°C for 2.5-min time interval

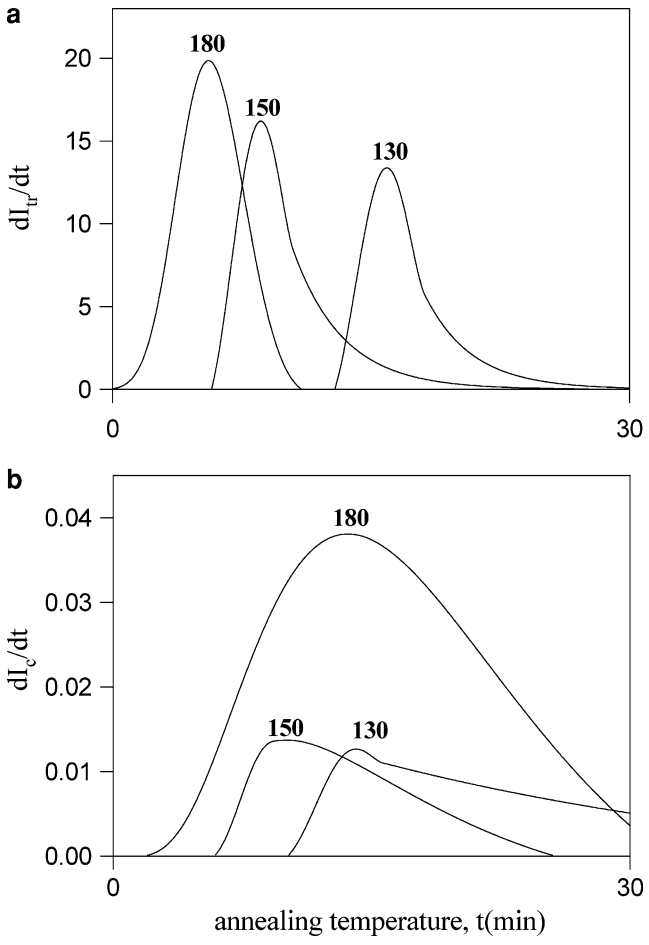

Fig. 12 First derivatives of **a** I_{tr}, **b** I_c at various temperatures

323°nm are shown in Fig. 2, where it is seen that I_F increased continuously by increasing the total annealing times. The behavior of transmitted and emission light intensities, I_{tr} and I_F, versus annealing time are plotted in Figs. 3a–c and 4a–c for the film samples annealed separately at 130, 150 and 180°C, respectively. It is seen that at an early stage of annealing, I_{tr} and I_F start to increase above a certain onset annealing time, called void closure time, t_v, for all film samples. t_v moved to the low annealing time region as the annealing temperature is increased. The increase in I_{tr} and I_F with increasing number of annealing time intervals can be explained first by the void closure process between particles, i.e. PS start to flow upon annealing and voids between particles can be filled. Later, however, both I_{tr} and I_F saturate by increasing annealing time indicating that the void closure process is completed. Further annealing makes the PS film semi transparent to light due to the interdiffusion of polymer chains across particle-particle interfaces where PS material percolates. It is also seen from Fig. 2 that scattered intensity, I_s decreases with increasing annealing time, t. The I_s is useful as a correction factor for the I_F intensity due to surface inhomogeneties. The behaviour of I_s and I_F/I_s are plotted in Figs. 5 and 6 with respect to annealing time, t.

The variation in I_F/I_s and I_{tr} depends on the mean free $< a >$ and optical path, s, of a photon in the film. The optical path is directly proportional to the probability of the photon encountering a pyrene molecule. Cartoon representation of film formation from latex particles is given in Fig. 7. Figure 7a shows that at the early stage of film formation, the powder film possesses

Table 2 Comparison of experimentally measured critical times t_r, and t_c with void closure time, t_v

Temp(°C)	130	140	150	160	170	180
t_r	15.9	11.5	9.6	7.3	6.1	5.6
t_v	12.5	10.0	7.5	5.0	5.0	2.5
t_c	14.1	19.9	10.1	17.9	7.1	13.6

many voids ($t = 0$). At this stage the film scatters the light totally yielding low I_{tr} and I_F. Figure 7b presents a film in which, due to the annealing, interparticle voids disappear ($t = t_v$). As soon as the voids are filled healing process takes place. Figure 7c presents a film where particle–particle boundaries have almost disappeared ($t = t_c$, $t = t_r$) and percolation cluster is formed. Finally, Fig. 7d shows the transparent film. Figure 8 presents the SEM micrographs of PS latex film at various annealing steps confirming the above picture.

In order to quantify the I_{tr} and I_F/I_s data and to explain the percolation behavior of the latex film formation phenomenon, the time derivative of I_{tr} and I_F/I_s are taken. The time derivative of the I_{tr} looks like a typical critical peak as plotted in Fig. 9 for the film sample annealed at 130°C. The position of the maximum of d I_{tr}/d t curve in Fig. 9 may correspond to the critical point, t_r[24] . Indeed, one can determine the position of the t_r on the time axis with great precision, by assuming the following relation

$$|p - p_r| \alpha |t - t_r| \tag{3}$$

at least in a narrow region about the critical point.

The scaling forms for the quantity P_∞ near the percolation threshold, together with Eq. 3 yields,

$$I_{tr} \alpha P_\infty \alpha B(t - t_r)^\beta \tag{4}$$

Similarly the following relations can be written

$$|p - p_c| \alpha |t - t_c| \tag{5}$$

and

$$I_c \alpha P_\infty \alpha A(t - t_c)^\beta \tag{6}$$

where the corrected intensity $I_c = I_F / I_s$ was used. Here B and A are the proportionality factors. The double logarithmic plots of I_{tr} and I_c versus $|t - t_r|$ and $|t - t_c|$ for $t > t_r$ and $t > t_c$ were plotted to determine β values very accurately. The results are shown in Figs. 10 and 11, respectively for the film samples annealed at 130°C. The produced values of the critical exponents are given in Table 1. Good agreement with the known value ($\beta = 0.41$)[22] of the percolation exponents in three dimensions was observed for the I_{tr} and I_c data and found to be $\beta = 0.31 \mp 0.05$ and $\beta = 0.37 \mp 0.08$, respectively.

The critical times, t_r and t_c, produced from the position of first derivative of I_{tr} and I_c, are presented in Fig. 12a and b, respectively. The behavior of t_r and t_c values against annealing temperature is compared with t_v in Table 2. Here we have to mention that the statistical uncertainties on t_c are not as good as on t_r. The dI_c/d curves in Fig. 12b are much wider than the curves in Fig. 12a, indicating poor determination of t_c. These difficulties most probably stem from the nature of the fluorescence technique. It is seen that all critical times decrease as the annealing time is increased, indicating that early void closure and percolation cluster formation occur at higher temperatures.

In conclusion, this work has introduced a novel approach to latex film formation mechanism where both transmitted light and fluorescence intensities can be used to monitor the formation of percolation cluster during film formation.

References

1. Mohammadi N, Klein A, Sperling LH (1993) Macromolecules 26:1019
2. Sambasivan M, Sperling LH, Klein A (1995) Macromolecules 28:152
3. Pekcan Ö, Arda E, Kesenci K, Piskin E (1998) J Appl Polym Sci 68:1257
4. Sambasivan M, Klein A, Sperling LH (1995) J Appl Polym Sci 58:357
5. Wang Y, Winnik MA (1993) J Phys Chem 97:2507
6. Canpolat M, Pekcan Ö (1995) Polymer 36:4433
7. Canpolat M, Pekcan Ö (1995) Polymer 36:2025
8. Pekcan Ö, Canpolat M (1996) J. Appl. Polym. Sci. 59:1699
9. Guerro R (1990) R Macromol Symp 35:389
10. Kim KD, Sperling LH, Klein A (1993) Macromolecules 26:4624
11. Pekcan Ö, Winnik MA, Croucher MD (1990) Macromolecules 23:2673
12. Wang Y, Zhao CL, Winnik MA (1991) J. Chem. Phys. 95:2143
13. Wang Y, Winnik MA (1993) Macromolecules 26:1347
14. Canpolat M, Pekcan Ö, (1996) J Polym Sci Polym Phys Ed 34:691
15. Pekcan Ö, Arda E (2002) Encyclopedia of surface and colloid science. Marcel and Dekker, New York, p 2691
16. Pekcan Ö, Arda E, Bulmus V, Piskin E (2000) J Appl Polym Sci 77:866
17. Arda E, Özer F, Piskin E, Pekcan Ö (2001) J Coll Interface Sci 233:271
18. Arda E, Pekcan Ö (2001) Polymer 42:7419
19. Broadbent SR, Hammersley JM (1957) Proc. Camb. Phil. Soc 53:629
20. Sahimi M (1994) Applications of percolation theory. Taylor and Francis, London
21. Stauffer D, Coniglio A, Adam M (1982) Adv Polym Sci 44:103
22. Stauffer D, Aharony A (1992) Introduction to percolation theory. Taylor and Francis, London
23. Feder J (1988) Fractals. Plenum Press, New York (1988).
24. Kaya D, Pekcan Ö, Yılmaz Y (2003) Phase Transit 76(6):543